Int. J. Solids Structures, 1974,Vol. 10, pp. 1287–1305. Pergamon Press. Printed in Gt. Britain.

BIFURCATION BUCKLING OF SHELLS OF REVOLUTION INCLUDING LARGE DEFLECTIONS, PLASTICITY AND CREEP

DAVID BUSHNELL†

Lockheed Palo Alto Research Laboratory, 3251 Hanover Street,
Palo Alto, California 94304, U.S.A.

(*Received* 26 *December* 1973; *revised* 18 *March* 1974)

Abstract—A summary is first presented of the conceptual difficulties and paradoxes surrounding plastic bifurcation buckling analysis. Briefly discussed are nonconservativeness, loading rate during buckling, and the discrepancy of buckling predictions with use of J_2 flow theory vs J_2 deformation theory. The axisymmetric prebuckling analysis, including large deflections, elastic–plastic material behavior and creep is summarized. Details are given on the analysis of nonsymmetric bifurcation from the deformed axisymmetric state. Both J_2 flow theory and J_2 deformation theory are described. The treatment, based on the finite-difference energy method, applies to layered segmented and branched shells of arbitrary meridional shape composed of a number of different elastic–plastic materials. Numerical results generated with a computer program based on the analysis are presented for an externally pressurized cylinder with conical heads.

NOMENCLATURE

$[C]$	Plastic loading matrix, equation (6)
$[D]$	elastic constants defined in equations (7) and (17)
ε	total strain anywhere in the shell wall
E	elastic modulus
G	shear modulus $= E/[2(1+\nu)]$
I	identity matrix
$[K]$	integrated constitutive law—equations (23) and (24)
N, M	stress, moment resultants or number of degrees-of-freedom in prebuckling, stability problems
n	number of full circumferential waves
p	normal pressure, Fig. 1
q	dependent variables—displacements and Lagrange multipliers
δq	infinitesimal change in q
r	radius of parallel circle, Fig. 1
R	radius of curvature, Fig. 1
s	arc length along meridian or stress deviator, depending on context
W	work done by external forces
z	distance from reference surface, Fig. 1
e	reference surface strain
κ	reference surface change in curvature
ν	Poisson's ratio
σ	stress
$\bar{\sigma}$	effective stress, $\bar{\sigma} = (\sigma_1^2 + \sigma_2^2 - \sigma_1\sigma_2)^{\frac{1}{2}}$
θ	circumferential coordinate
ψ	energy gradient or shell wall rotation component, depending on context
β	meridional rotation

Superscripts

$(\,)'$	$= \mathrm{d}(\,)/\mathrm{d}s$
$(\cdot)$	$= \mathrm{d}(\,)/\mathrm{d}\theta$
(1), (2)	= first, second order terms in δq
T	thermal, or transpose of matrix

† Staff Scientist.

Subscripts

0, o	prebuckling
1	meridional
2	hoop
12	shear
f	fixed
s	secant
T	tangent
$(\ )_{,i}$	$\partial(\ )/\partial(\delta q_i)$.

INTRODUCTION

Summary

To date bifurcation buckling analyses involving plasticity have been applied to simple structures with uniform prestress. Basic conceptual difficulties have been cleared up and paradoxes resolved. It is now understood that the nonconservative nature of plastic flow does not prevent the use of bifurcation buckling analysis to predict instability failure of practical structures; the concept of consistent loading of the material in the transition from prebifurcation state to adjacent postbifurcation state permits the use of instantaneous prebifurcation material properties in the stability equations; and an investigation of the effect of very small initial imperfections on the collapse loads of cruciform columns indicates that the reduced shear modulus $\bar{G}$ obtained from deformation theory should be used in the stability equations even if there is no history of shear along the prebifurcation path.

With the high speed electronic computer it is now feasible to calculate elastic–plastic bifurcation buckling loads of rather complex structures. The purpose of this paper is to present the theory for nonsymmetric bifurcation buckling of axisymmetrically loaded branched shells of revolution, including large axisymmetric prebuckling deflections and elastic–plastic effects.

The problem of nonconservativeness

Systems involving plastic flow are nonconservative. The energy required to bring a structure from its prebifurcation state to an adjacent buckled state depends upon the path of transition if any of the material is loading into the plastic region. Hill[1, 2] has shown, however, that as long as the infinitesimal path is reasonably direct the variation in infinitesimal energy dissipation from one path to another consists of higher order terms only.

The problem of loading rate during buckling

Analysis of the bifurcation buckling of elastic–plastic structures dates back to 1889 when Engesser[3] presented his tangent modulus theory for columns and Considère[4] set forth the "effective" or "double" modulus theory based on the assumption that the column unloads elastically on the concave side during incipient buckling at a given load. In 1895 Engesser, who had assumed that the total load on the column remains constant during buckling, acknowledged error in his original theory and determined the general expression for the reduced modulus. In 1910 von Kármán[5] presented the Considère–Engesser theory again, with actual evaluation of the reduced modulus for rectangular and idealized H-sections and comparisons with tests. Until Shanley's paper appeared in 1947 [6], the reduced modulus or "double modulus" model was accepted as the exact theory of column action, even though the tangent modulus model gave better agreement with tests. Shanley[6] resolved the paradox in 1947, when he stated:

"... in the derivation of the reduced-modulus theory a questionable assumption was made. It was assumed, by implication at least, that the column remains straight while the axial load is increased to the predicted critical value, *after which* the column bends, or tries to bend, Actually, the column is free to 'try to bend' at any time. There is nothing to prevent it from bending *simultaneously* with increasing axial load. Under such a condition it is possible to obtain a nonuniform strain distribution without any strain reversal taking place."

In a discussion appended to Shanley's paper, von Kármán further clarified the theory stating,

"Both Engesser's and my own analyses of the problem were based on the assumption that the equilibrium of the straight column becomes unstable when there are equilibrium positions infinitesimally near to the straight equilibrium position *under the same axial load.* ... Mr. Shanley's analysis represents a generalization of the question.... What is the smallest value of the axial load at which a bifurcation of the equilibrium positions can occur, regardless of whether or not the transition to the bent position requires an increase of the axial load?"

In 1950 Duberg and Wilder[7] provided further insight into the problem by showing that for small, finite imperfections bending will take place immediately as the load is applied but that local unloading of the material will not occur until the column is subjected to a relatively large bending moment. For vanishingly small initial imperfections, finite bending of the column will start at the bifurcation load predicted by the tangent modulus theory. Elastic unloading will not occur, however, until a higher load at which the column has deformed a finite amount along the post-bifurcation load–deflection curve. Duberg and Wilder show that for practical engineering materials the maximum load carrying capability of the column is only slightly above the tangent modulus bifurcation point.

It is physically reasonable to extend the concept of "tangent modulus bifurcation" to buckling of two-dimensional structures–plates and shells. Experiments and analyses have been conducted for simple plates and shells in which the prebuckling state is characterized by uniform compressive stress (see, e.g. [8 –16]). The analyses just cited are based on the tangent modulus method. Sewell[17] gives a more extensive bibliography.

In 1972 Hutchinson[18] calculated axisymmetric collapse pressures of an elastic–plastic spherical shell with various axisymmetric imperfections. As the imperfection amplitude approaches zero the collapse load approaches a value very slightly above the tangent modulus bifurcation load calculated from J_2 flow theory for a perfect shell. In justifying the use of the tangent modulus approach to bifurcation problems in general, Hutchinson [19] in 1974 wrote:

"The bifurcation solution is a linear sum of the fundamental solution increment and the eigenmode. We can always include a sufficiently large amount of the fundamental solution increment relative to the eigenmode such that the bifurcation mode satisfies the total loading restriction. ... The confusion in bifurcation applications apparently stems from the misconception that when bifurcation occurs total loading will be violated. On the contrary, it is the total loading condition itself which supplies the constraint on the combination of fundamental solution increment and eigenmode which must pertain."

The "total loading" condition cited above justifies the use of the "tangent modulus" approach to bifurcation buckling problems of elastic–plastic shells. The fact that the collapse

load is only slightly above the bifurcation load for vanishingly small imperfections makes an elastic–plastic bifurcation stability analysis in principle just as suitable for design purposes as an elastic bifurcation stability analysis. For bifurcation buckling of general shells under combined loading, in which the stresses are nonuniform and in which the prebuckling solution may be characterized by regions which are elastic or unloading and other regions which are loading into the plastic range, the "total loading" condition enunciated by Hutchinson may be generalized by the statement that the rate of change of material properties or "tangent properties" in the prebifurcation analysis govern the eigenvalue analysis also.

The flow theory vs deformation theory paradox

During the years when plastic buckling of uniformly stressed plates and shells was first being investigated, a perplexing paradox became apparent: Theoretical considerations and direct experimental evidence indicates that for general load paths flow theory is correct while deformation theory is not. However, bifurcation buckling analyses based on deformation theory conform better to experimentally determined buckling loads than do such analyses based on flow theory. The discrepancy may have to do with whether or not the instantaneous yield surface has corners. Experimental evidence on this point is contradictory. Experiments by Smith and Almroth[20] indicate that the yield surface may develop a region of very high curvature which "smooths" out with time.

The discrepancy in the prediction of bifurcation buckling loads is most pronounced in the case of an axially compressed cruciform column, discussed by Drucker[21], Cicala[22], Bijlaard[23] and Onat and Drucker[12]. In this example the prebifurcation stress state is uniform compression while the bifurcation mode involves pure shear. In a flow theory involving a smooth yield surface the shear modulus remains elastic as the material of the column is uniformly compressed into the plastic range. Use of the deformation theory gives the instantaneous shear modulus

$$\bar{G} = \frac{G}{1 + 3G\left(\frac{1}{E_s} - \frac{1}{E}\right)}, \tag{1}$$

where E_s is the secant modulus. Since the predicted buckling stress is proportional to the effective shear modulus, the discrepancy in predicted bifurcation loads is governed by the difference between G and $\bar{G}$. Onat and Drucker resolved the paradox by showing that cruciform columns with very small initial twist distributions collapse at loads slightly above the bifurcation loads predicted with deformation theory. Apparently a very small amount of shearing strain in the prebifurcation solution suffices to reduce the effective shear modulus from the elastic value G to a value near that predicted by deformation theory.

Because of this extreme sensitivity of the shear modulus to small, imperfection-related shearing forces applied while the material is being stressed, nominally without shear, into the plastic range, the value of G_{eff} predicted by deformation theory is used in the J_2 flow theory bifurcation analysis presented herein. The purpose of this strategy is to eliminate much of the flow theory vs deformation theory discrepancy in buckling predictions while retaining a realistic model of the material submitted to reasonably general axisymmetric prebifurcation loading histories.

However, in cases involving no in-plane shear either in the prebuckling phase or in the buckling process, J_2 deformation theory still predicts lower bifurcation buckling loads than

does J_2 flow theory. The axisymmetric buckling analysis of a spherical shell presented by Hutchinson[18] is a good example. Since J_2 deformation theory has given better agreement with test results than has J_2 flow theory, and since the discrepancy is not entirely related to the difference in effective shear modulus, it is prudent to perform stability analyses using aoth theories in order to establish the sensitivity of the predictions to the two models. Therefore, a J_2 deformation theory option is included in the analysis presented here.

ANALYSIS

Axisymmetric prebuckling analysis

Details of the prebuckling analysis are given by Bushnell[24] and only the main features will be summarized here. The theory is valid for small strains and moderately large rotations. The material behavior is modeled either as nonlinear elastic (J_2 deformation theory with loading and unloading along the stress–strain curve) or by means of J_2 flow theory with isotropic strain hardening and secondary creep. The following summary corresponds to the J_2 flow theory option.

A system of N nonlinear equations

$$\psi_i(q_j) = 0 \qquad \begin{matrix} i = 1, 2, \ldots N \\ j = 1, 2, \ldots N \end{matrix} \tag{2}$$

is solved by the Newton–Raphson method. The quantity N is the number of degrees-of-freedom in the discrete model. For each Newton–Raphson iteration the equations

$$\sum_{j=1}^{N} \frac{\partial \psi_i}{\partial q_j} \Delta q_j = -\psi_i \qquad i = 1, 2, \ldots N \tag{3}$$

must be solved for the correction terms Δq_j. Iterations continue until $|\Delta q_j/q_j| < 0{\cdot}001$. In equations (2) and (3) q_j are the nodal point degrees-of-freedom; ψ_i is the gradient of the energy functional with respect to q_i:

$$\psi_i = \int_V \lfloor \sigma \rfloor \left\{ \frac{\partial \varepsilon}{\partial q_i} \right\} \mathrm{d}V - \frac{\partial W}{\partial q_i} \tag{4}$$

and $\partial \psi_i / \partial q_j$ is the (i,j)th element of the tangent stiffness matrix:

$$\frac{\partial \psi_i}{\partial q_j} = \int_V \left(\lfloor \sigma \rfloor \left\{ \frac{\partial^2 \varepsilon}{\partial q_i \, \partial q_j} \right\} + \left[\frac{\partial \varepsilon}{\partial q_j} \right] [I - C]^T [D] \left\{ \frac{\partial \varepsilon}{\partial q_i} \right\} \right) \mathrm{d}V - \frac{\partial^2 W}{\partial q_i \, \partial q_j}. \tag{5}$$

In equations (4) and (5) $\lfloor \ \rfloor$ and $\{ \ \}$ indicate row and column vectors consisting in this axisymmetric prebuckling analysis of two stresses (σ_1, σ_2) or strains $(\varepsilon_1, \varepsilon_2)$. Subscripts 1 and 2 denote "meridional" and "circumferential." The 2×2 matrix $[C]$ is filled with zeroes if the material is elastic or unloading. If the material is being loaded into the plastic region, $[C]$ is given by

$$[C] = \frac{\left\{ \dfrac{\partial \bar{\sigma}}{\partial \sigma} \right\} \lfloor \partial \bar{\sigma} / \partial \sigma \rfloor [D]}{H' + \lfloor \partial \bar{\sigma} / \partial \sigma \rfloor [D] \left\{ \dfrac{\partial \bar{\sigma}}{\partial \sigma} \right\}}. \tag{6}$$

The various parameters in equation (6) are

$$\bar{\sigma} \equiv [\sigma_1^2 + \sigma_2^2 - \sigma_1\sigma_2]^{1/2} \qquad [D] \equiv \frac{E}{1-\nu^2}\begin{bmatrix} 1 & \nu \\ \nu & 1 \end{bmatrix}$$
$$H' = EE_T/(E - E_T) \tag{7}$$

where E_T is the tangent modulus. The uniaxial stress–strain curve is modeled as a series of up to 50 straight line segments.

The quantity W in equations (4) and (5) is the work done by external forces. The stresses σ_1 and σ_2 are given by

$$\{\sigma\} = [\varepsilon - \varepsilon^P - \varepsilon^C - \varepsilon^T][D] \tag{8}$$

where superscripts P, C and T denote "plastic", "creep" and "thermal." The total strains ε_1, ε_2 are given at any point in the shell wall by

$$\varepsilon_\alpha = (e_\alpha - z\kappa_\alpha)/(1 + z/R_\alpha) \qquad \alpha = 1, 2 \tag{9}$$

where z is the distance from an arbitrarily located reference surface and

$$\begin{aligned} e_1 &= u' + w/R_1 + \beta^2/2 \\ e_2 &= ur'/r + w/R_2 \\ \kappa_1 &= w'' - u'/R_1 - u(1/R_1)' \\ \kappa_2 &= \beta r'/r \\ \beta &= w' - u/R_1 \\ (\ )' &\equiv \mathrm{d}(\ )/\mathrm{d}s. \end{aligned} \tag{10}$$

In this analysis and in the bifurcation buckling analysis the strain is assumed to be small, and the engineering concept of strain, "change in length/original length," is thus implied. The shell geometrical parameters and displacement components are shown in Fig. 1. In equation (10) derivatives of the dependent variables u and w are replaced by appropriate first and second order finite difference formulas for variable nodal point spacing. The "u" nodal points are located midway between "w" nodal points, as shown in Fig. 2. Lagrange multipliers are introduced to include constraint conditions. The subscripted variable q in equations (2) and (3) thus represents "u" and "w" nodal degrees-of-freedom and the Lagrange multipliers.

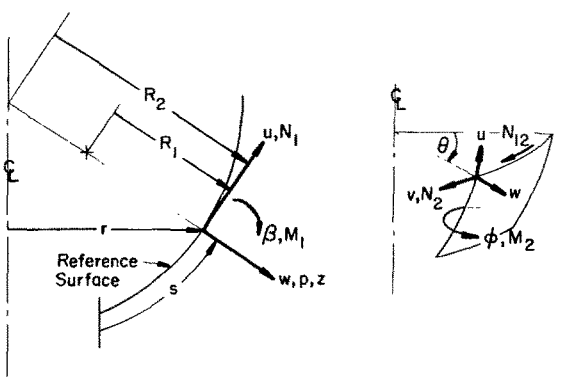

Fig. 1. Shell reference surface coordinates, geometry, displacements, stress resultants, pressure.

Integration with respect to the circumferential coordinate θ amounts to multiplication by 2π; integration along the meridian is replaced by multiplication by the arc length between two adjacent "u" nodes; and integration through the shell thickness is accomplished by Simpson's rule. The shell consists of up to 9 layers, each with a minimum of 5 integration points through its thickness, and each with its own stress–strain curve. The entire structure can consist of up to 25 segments branched in an arbitrary way as long as each segment has the same axis of revolution.

The prebuckling iteration strategy is as follows: At each load level there are two nested iteration loops. In the inner loop the set of simultaneous nonlinear algebraic equations (2) with given fixed material properties and plastic and creep strains is solved. This is the "Newton–Raphson loop". In the outer loop the strain-dependent material properties (the matrix $[C]$), the plastic strain components ε_1^P, ε_2^P and the creep strain components ε_1^C, ε_2^C are calculated. Double iterations at a given load level continue until the displacements no longer change. In this way the favorable convergence property of the Newton–Raphson procedure is preserved, equilibrium is satisfied within the degree of approximation inherent in a discrete model, and the flow law of the material is satisfied at every point in the structure. It has been found that the use of this strategy permits very big load steps, even if the material is loading plastically. A very complete description of the flow of calculations and many numerical examples are given in [24], including comparisons between flow theory and deformation theory, comparisons with test results, and charts showing how many iterations and how much computer time are required for solution of the nonlinear equations for several load increments.

Bifurcation buckling analysis

If q_0 represents an equilibrium state then $\psi_i(q_0) = 0$, $i = 1, 2 \ldots M$. (The number of degrees-of-freedom M in the stability analysis is more than the number of degrees-of-freedom N in the axisymmetric prebuckling analysis because nonsymmetric buckling modes are permitted). At the bifurcation load there exists a nontrivial infinitesimal displacement distribution δq, henceforth called the buckling mode, such that

$$\psi_i(q_0 + \delta q) = 0 \qquad i = 1, 2, \ldots M. \tag{11}$$

The ψ can be expanded in Taylor series about q_0, thus:

$$\psi_i(q_0 + \delta q) = \psi_i(q_0) + \sum_{j=1}^{M} \left(\frac{\partial \psi_i}{\delta(\delta q_j)}\right)_{\delta q \to 0} \delta q_j + \cdots = 0 \qquad i = 1,2, \ldots M \tag{12}$$

Since $\psi_i(q_0) = 0$ it follows that

$$\sum_{j=1}^{M} \left(\frac{\partial \psi_i}{\partial(\delta q_j)}\right)_{\delta q \to 0} \delta q_j = 0 \qquad i = 1, 2, \ldots M. \tag{13}$$

The criterion for the existence of a non-trivial vector δq is that the determinant of the $M \times M$ matrix $[\partial\psi/\partial(\delta q)]$, evaluated in the limit as $\delta q \to 0$, vanish.

The (i,j)th element of the stability matrix $[\partial\psi_i/\partial(\delta q_j)]_{\delta q \to 0}$ can be derived with use of equation (5) as a starting point. The stress and strain vectors $\lfloor\sigma\rfloor$, $\lfloor\varepsilon\rfloor$ will now contain three elements rather than two, since the buckling mode may be nonsymmetric:

$$\begin{aligned} \lfloor\sigma\rfloor &\equiv \lfloor\sigma_1, \sigma_2, \sigma_{12}\rfloor \\ \lfloor\varepsilon\rfloor &\equiv \lfloor\varepsilon_1, \varepsilon_2, \varepsilon_{12}\rfloor \end{aligned} \tag{14}$$

in which subscript $(\ )_{12}$ denotes shear. The material property matrix $[I - C]^T[D]$ must include shear stiffness elements not present in the axisymmetric prebuckling analysis. In accordance with the discussion of cruciform column buckling in the introduction, the effective shear modulus $\bar{G}$ predicted by deformation theory

$$G = 0.5E/(1 + \nu + g) \tag{15}$$

in which

$$g = 3(E/E_s - 1)/2 \tag{16}$$

is used if the material is loading plastically. The quantity E_s is the secant modulus determined from the axial stress–strain curve and regarded as a function of effective strain for biaxial stress. Of course, g is set equal to zero if the material has not yielded or is unloading. In equation (5) $[I]$ is the 3×3 identity matrix and $[C]$ and $[D]$ are given by

$$[C] = [0] \text{ if unloading or elastic}$$

$$[C] = \begin{bmatrix} c_{11} & c_{12} & 0 \\ c_{21} & c_{22} & 0 \\ 0 & 0 & 0 \end{bmatrix} \quad \text{if loading plastically} \tag{17}$$

$$[D] = \frac{E}{1 - \nu^2} \begin{bmatrix} 1 & \nu & 0 \\ \nu & 1 & 0 \\ 0 & 0 & \dfrac{(1 - \nu^2)}{2(1 + \nu + g)} \end{bmatrix}.$$

The elements c_{11}, c_{12}, c_{21}, c_{22} of $[C]$ are given by equation (6).

The strains ε_1, ε_2 and ε_{12} correspond to the total deformations-finite prebuckling u_0, w_0 plus infinitesimal buckling δu, δv, δw. The meridional and circumferential strains vary through the shell wall thickness according to equation (9) and the shear strain varies according to

$$\varepsilon_{12} = (e_{12} + 2z\kappa_{12})/[(1 + z/R_1)(1 + z/R_2)]^{1/2}. \tag{18}$$

The volume element $\mathrm{d}V$ is

$$\mathrm{d}V = r(1 + z/R_1)(1 + z/R_2)\mathrm{d}z\, \mathrm{d}\theta\, ds. \tag{19}$$

The reference surface strains e and changes in curvature κ in terms of the total displacements u, v, w are:

$$\begin{aligned} e_1 &= u' + w/R_1 + \tfrac{1}{2}(\beta^2 + \gamma^2) \\ e_2 &= \dot{v}/r + ur'/r + w/R_2 + \tfrac{1}{2}(\psi^2 + \gamma^2) \\ e_{12} &= \dot{u}/r + r(v/r)' + \beta\psi \\ \kappa_1 &= \beta' \\ \kappa_2 &= \dot{\psi}/r + r'\beta/r \\ \kappa_{12} &= 2(-\dot{\beta}/r + r'\psi/r + v'/R_2) \end{aligned} \tag{20}$$

in which

$$\begin{aligned} u &= u_0 + \delta u \\ v &= v_0 + \delta v \qquad (v_0 = 0 \text{ in this analysis}) \\ w &= w_0 + \delta w \\ \beta &= w' - u/R_1 \\ \psi &= \dot{w}/r - v/R_2 \\ \gamma &= \tfrac{1}{2}(\dot{u}/r - v' - vr'/r). \end{aligned} \tag{21}$$

Primes indicate differentiation with respect to the meridional arc length s and dots indicate differentiation with respect to the circumferential coordinate θ. Positive u, v, w are shown in Fig. 1.

Use of equations (9, 14 and 17–19) in equation (5) and integration through the shell wall thickness leads to the following equation:

$$[\partial\psi_i/\partial(\delta q_j)]_{\delta q\to 0} = \left[\int_\theta\int_s (\lfloor S_0\rfloor\{e_{,ij}\} + \lfloor e_{,j}\rfloor[K]\{e_{,i}\})\right] r\,\mathrm{d}s\,\mathrm{d}\theta - W_{,ij}]_{\delta q\to 0} \tag{22}$$

where

$$\lfloor S_0\rfloor \equiv \lfloor N_{10}, N_{20}, N_{120}, M_{10}, M_{20}, M_{120}\rfloor \quad \text{(prebuckling stress resultants)}$$

$$(\ )_{,ij} \equiv \frac{\partial(\ )}{\partial(\delta q_i)\partial(\delta q_j)} \qquad (\ )_{,i} \equiv \frac{\partial(\ )}{\partial(\delta q_i)}$$

$$\lfloor e\rfloor \equiv \lfloor e_1, e_2, e_{12}, \kappa_1, \kappa_2, \kappa_{12}\rfloor$$

$$[K] \equiv \begin{bmatrix} K_{11} & K_{12} & 0 & K_{14} & K_{15} & 0 \\ K_{12} & K_{22} & 0 & K_{24} & K_{25} & 0 \\ 0 & 0 & K_{33} & 0 & 0 & K_{36} \\ K_{14} & K_{24} & 0 & K_{44} & K_{45} & 0 \\ K_{15} & K_{25} & 0 & K_{45} & K_{55} & 0 \\ 0 & 0 & K_{36} & 0 & 0 & K_{66} \end{bmatrix} \tag{23}$$

with

$$\begin{aligned} K_{11} &= \int E_{11}k_3\,\mathrm{d}z \qquad K_{22} = \int (E_{22}/k_3)\,\mathrm{d}z \qquad K_{12} = \int E_{12}\,\mathrm{d}z \\ K_{14} &= -\int E_{11}k_3 z\,\mathrm{d}z \qquad K_{15} = -\int E_{12}z\,\mathrm{d}z \\ K_{24} &= -\int E_{12}z\,\mathrm{d}z \qquad K_{25} = -\int E_{22}/k_3)z\,\mathrm{d}z \\ K_{33} &= \int G_{\mathrm{eff}}\,\mathrm{d}z \qquad K_{36} = \int G_{\mathrm{eff}}z\,\mathrm{d}z \qquad K_{66} = \int G_{\mathrm{eff}}z^2\,\mathrm{d}z \end{aligned} \tag{24}$$

($G_{\mathrm{eff}} = G$ for unloading; $\bar{G}$ for plastic loading)

$$K_{44} = \int E_{11}k_3 z^2\,\mathrm{d}z \qquad K_{45} = \int E_{12}z^2\,\mathrm{d}z \qquad K_{55} = \int (E_{22}/k_3)z^2\,\mathrm{d}z$$

in which

$$k_3 = (1 + z/R_2)/(1 + z/R_1)$$
$$k_3 = (1 + z/R_1)/(1 + z/R_2), \tag{25}$$

and

$$E_{11} = \frac{E}{1 - \nu^2}(1 - c_{11} - \nu c_{21}) \qquad E_{22} = \frac{E}{1 - \nu^2}(1 - \nu c_{12} - c_{22})$$
$$E_{12} = \frac{E}{1 - \nu^2}(\nu - c_{12} - \nu c_{22}) \tag{26}$$

where the c_{ij} are given by equation (6). Equations (26) correspond to J_2 flow theory.

If J_2 deformation theory is used equations (26) must be replaced by

$$E_{11} = a/(a^2 - b^2) \qquad E_{12} = -b/(a^2 - b^2) \qquad E_{22} = E_{11} \tag{27}$$

in the prebuckling analysis and by

$$E_{11} = \frac{c_s}{a_s c_s - b_s^2} \qquad E_{12} = \frac{-b_s}{a_s c_s - b_s^2} \qquad E_{22} = \frac{a_s}{a_s c_s - b_s^2} \tag{28}$$

in the bifurcation buckling analysis. The quantities a, b, a_s, b_s and c_s are given by

$$a = 1/E_s \qquad b = -\frac{1}{E}(\nu + g/3)$$
$$a_s = a + g' s_1^2/E \qquad b_s = b + g' s_1 s_2/E \qquad c_s = a + g' s_2^2/E \tag{29}$$

in which g is given by equation (16) and

$$s_1 = (2\sigma_1 - \sigma_2)/3 \qquad s_2 = (2\sigma_2 - \sigma_1)/3$$
$$g' \equiv \frac{dg}{dJ_2} = \frac{9}{4}\left(\frac{E}{E_T} - \frac{E}{E_s}\right)\Big/(\sigma_1^2 + \sigma_2^2 - \sigma_1\sigma_2). \tag{30}$$

It is clear that in equations (20) only the terms quadratic in the infinitesimal displacements δu, δv, δw contribute to the first term of the (i,j)th stability matrix element (equation 22) and only the terms linear in δu, δv, δw contribute to the second term in equation (22). The quantity W_{ij} represents the second derivative of the live load (pressure–rotation) effect which is given by

$$-W = \int_\theta \int_s \left([\delta u, \delta v, \delta w] \begin{bmatrix} -p/R_1 & 0 & -p' \\ 0 & -p/R_2 & \\ -p' & 0 & p\left(\frac{1}{R_1} + \frac{1}{R_2}\right) \end{bmatrix} \begin{Bmatrix} \delta u \\ \delta v \\ \delta w \end{Bmatrix} \right) r \, ds \, d\theta \tag{31}$$

where p and p' are the normal pressure distribution and its meridional derivative.

The buckling mode δq or δu, δv, δw is assumed to vary harmonically around the circumference with a single harmonic, so that θ-differentiation in equations (20) and (21) can be replaced by multiplication by n or $-n$, where n is the number of full circumferential waves. Hence the θ-integration in equation (22) can be replaced by multiplication by 2π if $n = 0$

and by π otherwise. As in the prebuckling analysis, integration along the meridional arc s is replaced by multiplication by the distance $\Delta s_i = l_i$ (Fig. 2) between two adjacent nodes u_i and u_{i+1}. Corresponding to the ith meridional "finite difference element" [25] the reference surface strains e and changes in curvature κ as well as the prebuckling stress resultants $[S_0]$ are evaluated halfway between u_i and u_{i+1} in terms of the seven nodal point variables w_{i-1}, $u_i, v_i, w_i, u_{i+1}, v_{i+1}, w_{i+1}$. Figure 2 shows the arrangement of nodes and their relationship to the integration area and the location "E" at which the second variation of the energy (equation 22) is evaluated.

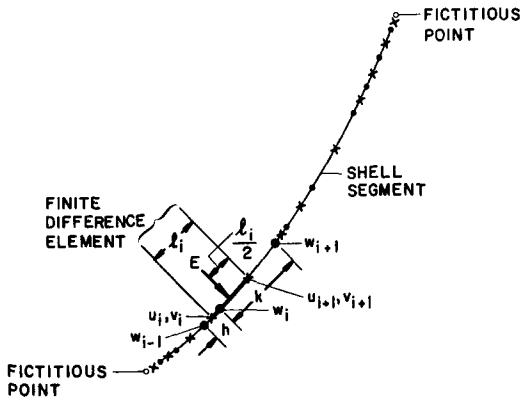

Fig. 2. Arrangement of nodes for the bifurcation buckling analysis.

The total reference surface strains and changes in curvature can be expressed in terms of three parts

$$\lfloor e \rfloor = \lfloor e^{(0)} \rfloor + \lfloor e^{(1)} \rfloor + \lfloor e^{(2)} \rfloor \tag{32}$$

where superscripts $^{(i)}$, $i = 0, 1, 2$ indicate zeroth, first and second order in the buckling displacements δq or δu, δv, δw. The zeroth order represents the axisymmetric prebuckled state. The first and second order terms are given by

$$\{e^{(1)}\} = \begin{Bmatrix} e_1^{(1)} \\ e_2^{(1)} \\ e_{12}^{(1)} \\ \kappa_1^{(1)} \\ \kappa_2^{(1)} \\ \kappa_{12}^{(2)} \end{Bmatrix} = \begin{Bmatrix} (\delta u)' + \delta w/R_1 + \beta_0 \delta\beta \\ -n\delta v/r + r'\delta u/r + \delta w/R_2 \\ n\delta u/r + r(\delta v/r)' + \beta_0 \delta\psi \\ (\delta\beta)' \\ -n\delta\psi/r + r'\delta\beta/r \\ 2(-n\delta\beta/r + r'\delta\psi/r + (\delta v)'/R_2) \end{Bmatrix} \tag{33}$$

$$\{e^{(2)}\} \equiv \begin{Bmatrix} e_1^{(2)} \\ e_2^{(2)} \\ e_{12}^{(2)} \\ \kappa_1^{(2)} \\ \kappa_{12}^{(2)} \\ \kappa_{12}^{(2)} \end{Bmatrix} = \begin{Bmatrix} \frac{1}{2}[(\delta\beta)^2 + (\delta\gamma)^2] \\ \frac{1}{2}[(\delta\psi)^2 + (\delta\gamma)^2] \\ \delta\beta\delta\psi \\ 0 \\ 0 \\ 0 \end{Bmatrix}. \tag{34}$$

In the derivation of equation (33) it has been assumed that δu and δw vary as $\sin\theta$ around

the circumference and δv varies as $\cos n\theta$. Two of the prebuckling rotation components, ψ_0 and γ_0, are zero.

Equations (21) can be used to express $\delta\beta$, $\delta\psi$ and $\delta\gamma$ in terms of δu, δv, δw. Given the nodal point arrangement shown in Fig. 2 and the fact that the second variation of the energy $\partial\psi/\partial(\delta q)$ is evaluated at the point marked "E", the buckling displacements and their derivatives are written in terms of the nodal point values thus:

$$\delta u = (\delta u_i + \delta u_{i+1})/2 \qquad \delta v = (\delta v_i + \delta v_{i+1})/2$$

$$(\delta u)' = (\delta u_{i+1} - \delta u_i)/l_i \qquad (\delta v)' = (\delta v_{i+1} - \delta v_i)/l_i$$

$$\begin{Bmatrix} \delta w \\ (\delta w)' \\ (\delta w)'' \end{Bmatrix} = \begin{bmatrix} a_{11} & a_{12} & a_{13} \\ a_{21} & a_{22} & a_{23} \\ a_{31} & a_{32} & a_{33} \end{bmatrix} \begin{Bmatrix} \delta w_{i-1} \\ \delta w_i \\ \delta w_{i+1} \end{Bmatrix} \tag{35}$$

where

$$\begin{aligned} a_{11} &= (h-k)(3k+h)/[16(h^2+hk)] \\ a_{12} &= (h+3k)(3h+k)/(16hk) \\ a_{13} &= (k-h)(3h+k)/[16(k^2+hk)] \\ a_{21} &= -1/2h \qquad a_{22} = (1/2h - 1/2k) \qquad a_{23} = 1/2k \\ a_{31} &= 2/[h(h+k)] \\ a_{32} &= -2/(hk) \\ a_{33} &= 2/[k(h+k)]. \end{aligned} \tag{36}$$

The quantities h and k are shown in Fig. 2. With appropriate substitutions involving equations (21) and (35), equation (33) assumes the form:

$$\{e^{(1)}\}_i = ([B_1] + \beta_0[B_2])_i\{\delta q\}_i \tag{37}$$

in which i indicates "ith finite difference element" and

$$\lfloor \delta q \rfloor_i \equiv \lfloor w_{i-1}, u_i, v_i, w_i, u_{i+1}, v_{i+1}, w_{i+1} \rfloor. \tag{38}$$

The 6×7 matrices $[B_1]$ and $[B_2]$ are functions of the shell geometry, circumferential wave number n and the mesh spacing parameters h and k. If the mesh spacing is constant these matrices are given by equations (14) and (15) of [26].

The first term on the right hand side of equation (22) is the second derivative with respect to the ith and jth nodal degrees-of-freedom of $[S_0]\{e^{(2)}\}$, with $\{e^{(2)}\}$ given by equation (34). It can be easily shown that

$$\lfloor S_0 \rfloor \{e^{(2)}\} = \lfloor \delta q \rfloor [R]^T [N_0][R]\{\delta q\} \tag{39}$$

where

$$[N_0] \equiv \begin{bmatrix} N_{10} & N_{120} & 0 \\ N_{120} & N_{20} & 0 \\ 0 & 0 & (N_{10} + N_{20}) \end{bmatrix} \tag{40}$$

and $[R]$ is the matrix relating rotations to nodal point displacements:

$$\begin{Bmatrix} \delta\beta \\ \delta\psi \\ \delta\gamma \end{Bmatrix} = [R]\{\delta q\}. \tag{41}$$

If the mesh spacing is constant the 3×7 matrix $[R]$ is given by equation (16) of [26]. In this analysis the prebuckling shear resultant N_{120} is zero. Before differentiation with respect to the ith and jth nodal degrees-of-freedom the second term on the right-hand side of equation (22) can be written in the form

$$\lfloor e^{(1)} \rfloor [K] \{e^{(1)}\} = \lfloor \delta q \rfloor ([B_1] + \beta_0 [B_2])^T [K] ([B_1] + \beta_0 [B_2]) \{\delta q\}. \tag{42}$$

If

$$\lfloor \delta u, \delta v, \delta w \rfloor = [U] \{\delta q\} \tag{43}$$

and $[P]$ is the 3×3 matrix given in equation (31), then before differentiation the third term on the right-hand side of equation (22) is given by

$$-W = \lfloor \delta q \rfloor [U]^T [P] [U] \{\delta q\} \tag{44}$$

where $[U]$ is a 3×7 matrix easily derived from equations (35). If the shell is considered to be loaded by two "sets" of forces, one set fixed and the other set varying, the complete stiffness matrix of the ith shell element can be written in the form

$$[H]_i = \pi r_i l_i (([B_1] + \beta_{0f}[B_2])^T [K] ([B_1] + \beta_{0f}[B_2]) + [R]^T [N_{0f}] [R] + [U]^T [P_f] [U]$$
$$\lambda [([B_1]^T [K] [B_2] + [B_2]^T [K] [B_1]) \beta_0 + [R]^T [N_0] [R] + [U]^T [P] [U]] + \lambda^2 [B_2)^T [K] [B_2] \beta_0{}^2)_i. \tag{45}$$

Subscript i denotes evaluated at the point "E" of the ith finite difference element, f denotes "fixed" or "not an eigenvalue parameter", and λ is the eigenvalue parameter.

The global stiffness matrix is calculated by appropriate superposition of the local 7×7 matrices $[H]_i$, $i = 1, 2, \ldots L$, where L is the total number of finite difference elements in the structure. Boundary conditions and juncture conditions for compatibility between shell segments are handled by the introduction of Lagrange multipliers. A complete description is presented in [26]. Examples of the configuration of stiffness matrices for branched shells are shown in [27]. A more complete description of the derivation of the stiffness matrix is given in [28].

The values of λ that cause the determinant of the global stiffness matrix to vanish correspond to bifurcation points on the load–deflection curve, with plasticity effects included in the model.

"Consistent" loading model: A further justification

Throughout the derivation of the stiffness matrix it has been assumed that the constitutive equation coefficients $[K]$ are independent of the infinitesimal buckling displacements δq. This assumption is in accordance with the "total" or "consistent" loading principle enunciated in the introduction. To reiterate—"consistent" loading is taken to mean that if the material at a point in the shell is loading plastically before bifurcation, it will also do so in the transition δq to the buckled configuration. If the material is elastic before bifurcation, it will remain so during incipient buckling. In the introduction are quoted passages from the work of Shanley[6] and Hutchinson[19] which defend the consistent loading model. The following physical argument is presented to further justify it.

Let us hypothesize that the eigenvalue obtained from the consistent loading model is physically meaningless because a *finite* amount of material which has been loading into the plastic region suddenly unloads in the *infinitesimal* transition from the unbuckled state q to

the buckled configuration $q + \delta q$. The effect would be to produce a stiffer structure and hence, in the presence of a given prebuckling state, a higher eigenvalue than would result from the consistent loading model. Suppose also that an eigenvalue and corresponding kinematically admissible mode have been determined from the consistent loading model. Now assume that a new nonlinear equilibrium analysis is performed for the shell with an infinitesimal imperfection of the same shape as this buckling mode. Since the imperfection is infinitesimal the load–deflection behavior will differ from that of the perfect shell only infinitesimally for loads smaller than the lowest eigenvalue obtained from the consistent loading model. If, as hypothesized, this eigenvalue were physically meaningless and the true bifurcation point lies a finite load increment above it, then the material of the infinitesimally imperfect shell would continue to load consistently right through the neighborhood of the bifurcation load calculated by means of the consistent loading model. A contradiction therefore exists: It has just been hypothesized that the eigenvalue from the consistent loading model is physically meaningless because *infinitesimal* perturbations of the form of the buckling mode cause a *finite* amount of the material to unload suddenly. However, the material of an actual shell containing such a perturbation in geometry loads consistently at the eigenvalue calculated from the consistent loading model. Therefore, this eigenvalue must be physically meaningful and must correspond to a bifurcation point on the load–deflection curve of the perfect shell.

NUMERICAL RESULTS

A computer program called BOSOR5 has been written based on the analysis just described. Both J_2 flow theory and J_2 deformation theory are provided as alternate branches. This program is an extended version of BOSOR4 [28]. The results discussed in the following paragraphs were obtained with the J_2 flow theory option of BOSOR5.

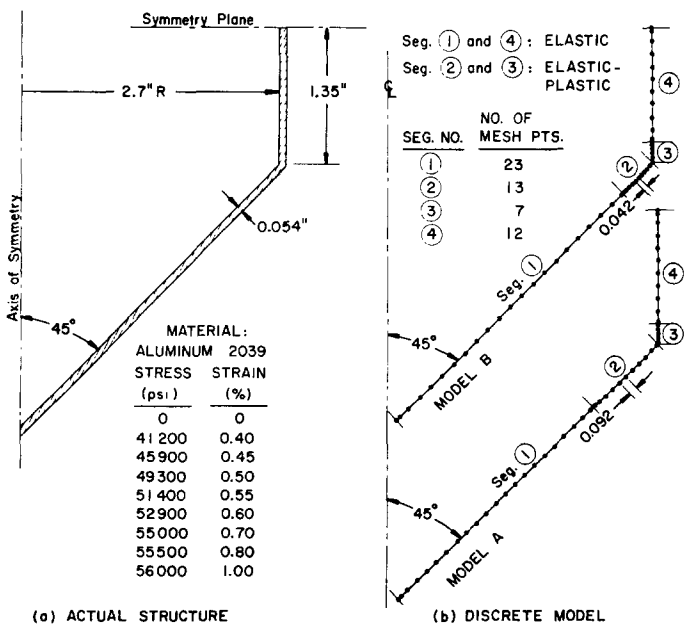

Fig. 3. Aluminum pressure vessel and discrete models.

Figure 3(a) shows part of an aluminum shell which is submitted to uniform external pressure. The stress–strain curve is modeled as a series of straight line segments passing through the data points listed in the figure. Half of the shell (from the apex of the cone to the symmetry plane of the cylinder) is modeled as shown in Fig. 3(b). The region which becomes plastic is confined to the neighborhood of the juncture between the cone and cylinder. Computer time is saved by division of the cone and cylinder into two segments each—an elastic segment and an elastic–plastic segment.

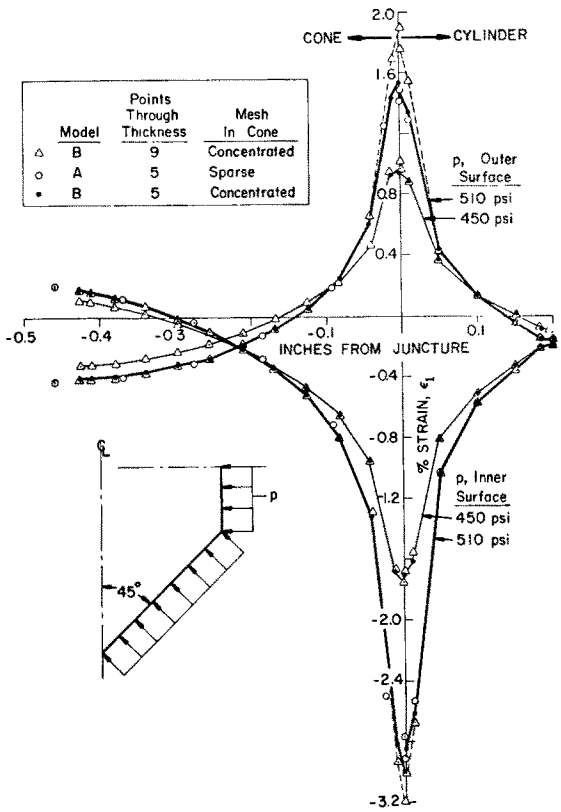

Fig. 4. Meridional strains near cylinder–cone juncture.

Figure 4 shows the sensitivity of the prebuckling axisymmetric meridional strain distributions near the juncture to changes in the nodal point density and the number of integration stations taken through the wall thickness. Figure 5 shows the reduction of the wall stiffness near the juncture just before bifurcation buckling. The reference surface is the inner surface.

The minimum predicted buckling pressure corresponds to 6 circumferential waves and is 511 psi for Model A with 5 integration points through the thickness, 512 psi for Model A with 9 integration points, and 515 psi for Model B with 5 integration points.

If the material is assumed to remain elastic the analysis with Model A yields a minimum buckling pressure of 565 psi. An elastic model with meridional moment-carrying capability across the juncture in the prebuckling analysis but with a hinge there in the stability analysis,

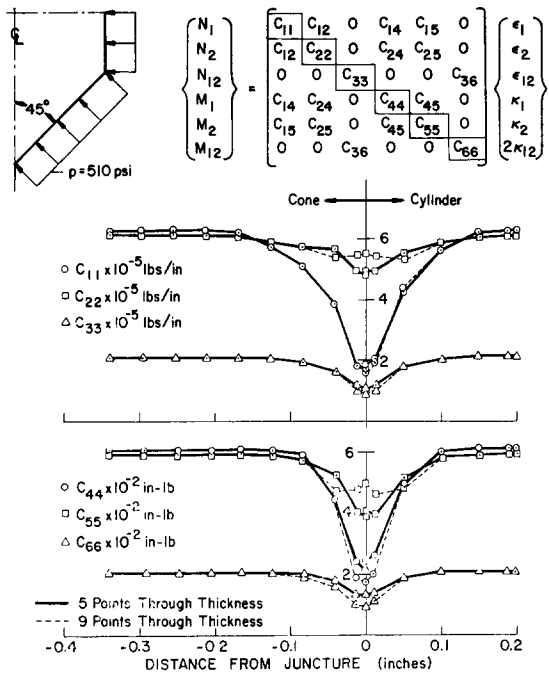

Fig. 5. Shell wall stiffness coefficients near cylinder–cone juncture.

yields a predicted critical pressure of 533 psi. An elastic model with a hinge assumed at the juncture in both the prebuckling and the stability analyses gives 481 psi for the buckling pressure. All critical pressures correspond to 6 circumferential waves. Figure 6 shows three of the four buckling modes.

Figure 7 and Table 1 demonstrate the strategy used in BOSOR5 for obtaining bifurcation buckling loads. At a given circumferential wave number n_0 the load is increased in steps until the stability determinant changes sign. Then the load step is automatically reduced by a factor of 10 and the process repeated, starting from the previous load as shown in Fig. 7.

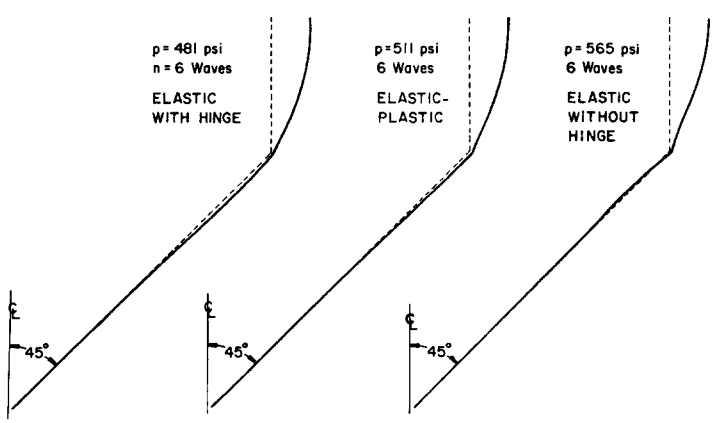

Fig. 6. Buckling modes with various models.

Corresponding to the point labeled (4), for which it is known that with $n = n_0$ the buckling pressure is between 510 and 515 psi, an eigenvalue problem of the form shown in equation (45) is set up. The quantities β_{0f}, N_{0f} and P_f in equation (45) correspond to the "fixed" prebuckled state of 510 psi, and β_0, N_0 and P correspond to the increments in prebuckling rotation, stress resultants, and pressure distribution for a 5-psi increment in external pressure added to the "fixed" 510 psi. The circumferential wave number n is varied until a minimum eigenvalue λ is found.

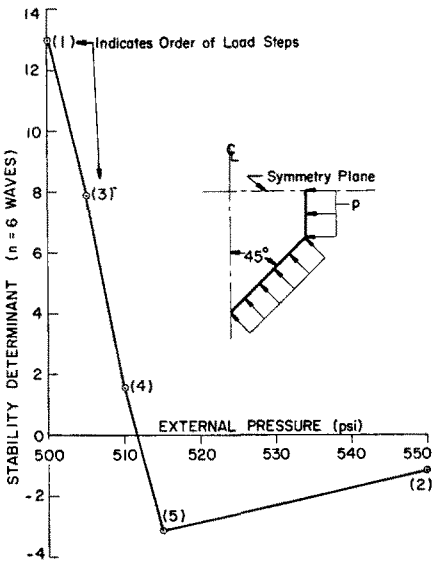

Fig. 7. Finding the lowest eigenvalue.

In Table 1 the terminology "trial" is used. A "trial" is defined as a solution of the nonlinear algebraic equations (2) for given material properties and estimates of the plastic and creep strain components. At 300 psi three trials were required for complete convergence of the prebuckling analysis.

The entries in Table 1 associated with ($n = 5$) require an explanation: The "stability stiffness matrix" is the global matrix composed of all terms in equation (45) not multiplied by λ or λ^2; the "load geometric matrix" is composed of the terms multiplied by λ; and the "lambda-squared" matrix is composed, not surprisingly, of the terms multiplied by λ^2. Eigenvalues are extracted by the inverse power iteration method with spectral shifts. The solution of the quadratic eigenvalue problem is described in [28].

Further numerical results and comparisons with tests are given in a sequel to this paper, also published in this journal.

Acknowledgements—The author appreciates the helpful discussions and encouragement of Bo O. Almroth John W. Hutchinson and Phil Underwood. This work was jointly sponsored by the Lockheed Independent Research Program and the Department of Structural Mechanics of the Naval Ship Research and Development Center under Naval Ship Systems Command, Operation and Maintenance Navy Fund, Contract N00014-73-C-0065. Dr. Rembert Jones and Miss Joan Roderick were technical monitors.

Table 1. Summary of calculations and UNIVAC 1108/EXEC8 computer times for 45-degree specimen elastic–plastic bifurcation buckling analysis (137 degrees of freedom in prebuckling analysis, 201 in stability analysis)

Pressure (psi)	Calculations in progress	Elapsed time (sec)
0	input data read in, preliminary calculations finished	3·237
300	trial #1 completed. 4 Newton–Raphson iterations required	5·482
300 prebuckling	trial #2 completed. 2 Newton–Raphson iterations required	6·812
300 analysis	trial #3 completed. 1 Newton–Raphson iteration required, list	10·454
300 ($n=6$)	stability stiffness matrix for $n=6$ waves computed	11·268
300 ($n=6$)	stability determinant calculated	11·684
350 ($n=6$)	three trials, 6 *N–R* iterations, stability analysis completed	19·528
400 ($n=6$)	four trials, 8 *N–R* iterations, stability analysis completed	28·721
450 ($n=6$)	four trials, 8 *N–R* iterations, stability analysis completed	38·231
500 ($n=6$)	four trails, 8 *N–R* iterations, stability analysis completed	48·136
550 ($n=6$)	four trials, 8 *N–R* iterations, stability analysis completed (stability determinant changes sign between 500 and 550 psi)	58.711
505 ($n=6$)	two trials, 3 *N–R* iterations, stability analysis completed	64·737
510 ($n=6$)	three trials, 5 *N–R* iterations, stability analysis completed	72·902
515 ($n=6$)	two trials, 3 *N–R* iterations, stability analysis completed (stability determinant changes sign between 510 and 515 psi)	78·140
510	two trials, 3 *N–R* iterations, list	82·981
510 ($n=5$)	stability stiffness matrix for $n=5$ waves computed	83.761
510 ($n=5$)	load-geometric matrix for $n=5$ waves computed	84·661
510 ($n=5$)	lambda-squared matrix for $n=5$ waves computed	85·029
510 ($n=5$)	smallest eigenvalue for $n=5$ waves computed (two spectral shifts and a total of 12 inverse power iterations. Eigenvalue = 9·137, indicating that for $n=5$ waves the buckling pressure is $510+(515-510)\times 9{\cdot}137=555{\cdot}7$ psi	89·467
510 ($n=6$)	stability stiffness, load-geometric, lamba-squared matrices computed	92·075
510 ($n=6$)	smallest eigenvalue of $n=6$ waves computed (one shift, 4 power iterations required. Eigenvalue = 0·1516, indicating that the buckling pressure is $510+(515-510)\times 0{\cdot}1516=510{\cdot}8$	94·273
510 ($n=7$)	stability stiffness, load-geometric, lambda-squared matrices computed	96·881
510 ($n=7$)	smallest eigenvalue for $n=7$ waves computed (one shift, 5 power iterations. Eigenvalue = 3·63, therefore buckling pressure for $n=7$ is $510+(515-510)\times 3{\cdot}63=528{\cdot}2$	99·680

Minimum buckling pressure corresponds to $n=6$ waves and is 510·8 psi.

REFERENCES

1. R. Hill, A General Theory of Uniqueness and Stability in Elastic–Plastic Solids, *J. Mech. Phys. Solids* **6**, 236 (1958).
2. R. Hill, Some basic principles in the mechanics of solids without a natural time, *J. Mech. Phys. Solids* **7**, 209, (1959).
3. F. Engesser, Ueber die Knickfestigkeit Geradu Sträbe, *Z. Architektur Ingenieurwesen* **35**, 455 (1889).
4. A. Considère, Resistance des Pieces Comprimees, *Congres Int. Procedes de Construction*, p. 371. Annexe, Librairie Polytechnique, Paris (1891).
5. Th. von Kármán, Untensuchungen uder Knickfestigkeit, Mitteilungen uder Forschungsarbeiten, *Verein Deutsc. Ing.* **81** (1910).
6. F. R. Shanley, Inelastic column theory, *J. Aero. Sci.* **14**, 261 (1947).
7. J. E. Duberg and T. W. Wilder, III, Column behavior in the plastic stress range, *J. Aero. Sci.* **17**, 323 (1950).

8. G. H. Handelman and W. Prager, Plastic buckling of a rectangular plate under edge thrusts, *NACA TN* 1530, (August 1948).
9. E. Z. Stowell, A unified theory of plastic buckling of columns and plates, *NACA TN* 1556, (April 1948).
10. P. P. Bijlaard, Theory and tests on the plastic stability of plates and shells, *J. Aero. Sci.* **16**, 529 (1949).
11. S. B. Batdorf, Theories of plastic buckling, *J. Aero. Sci.* **16**, 405 (1949).
12. E. T. Onat and D. C. Drucker, Inelastic instability and incremental theories of plasticity, *J. Aero. Sci.* **20**, 181 (1953).
13. R. A. Pride and G. J. Heimerl, Plastic buckling of simply-supported compressed plates, *NACA TN* 1817, (April 1949).
14. R. M. Jones, Plastic buckling of eccentrically stiffened circular cylindrical shells, *AIAA Journal* **5**, 1147 (1967).
15. S. C. Batterman, Tangent modulus theory for cylindrical shells: buckling under increasing load, *Int. J. Solids Struct.* **3**, 501 (1967).
16. S. C. Batterman, Plastic stability of spherical shells, *J. Engng Mech. ASCE* **EM2**, 433 (1969).
17. M. J. Sewell, A survey of plastic buckling, *Stability*, edited by H. Leipholz, Chap 5, p. 85 (1972).
18. J. W. Hutchinson, On the postbuckling behavior of imperfection-sensitive structures in the plastic range, *J. Appl. Mech.* **39**, 155 (1972).
19. J. W. Hutchinson, Plastic buckling, *Advances in Applied Mechanics*, Vol 14, edited by C. S. Yih. Academic Press, New York (1974).
20. S. Smith and B. O. Almroth, An experimental investigation of plastic flow under biaxial stress, *Exp. Mech.* (June 1970).
21. D. C. Drucker, A discussion of theories of plasticity, *J. Aero. Sci.* **16**, 567 (1949).
22. P. Cicala, On the plastic buckling of a compressed strip, *J. Aero. Sci.* **17**, 378 (1950).
23. P. P. Bijlaard, On the plastic buckling of plates, *J. Aero. Sci.* **17**, 742 (1950).
24. D. Bushnell, Large deflection elastic–plastic creep analysis of axisymmetric shells, *Numerical solution of nonlinear structural problems*, AMD-Vol. 6, p. 103 (1973) (Published by the ASME).
25. D. Bushnell, Finite-difference energy models versus finite-element models: Two variational approaches in one computer program, *Numerical and Computer Methods in Structural Mechanics*, edited by S. J. Fenves, N. Perrone, A. R. Robinson and W. C. Schnobrich, p. 291. Academic Press, New York (1973).
26. D. Bushnell, Analysis of buckling and vibration of ring-stiffened, segmented shells of revolution, *Int. J. Solids Struct.* **6**, 157 (1970).
27. D. Bushnell, Stress, Stability, and vibration of complex, branched shells of revolution, AIAA Paper No. 73-360, AIAA/ASME/SAE 14th Structures, Structural Dynamics, and Material Conference, Williamsburg, Virginia, March 1973, *J. Computers & Structures*, **4**, 399 (1974).
28. D. Bushnell, Stress, stability and vibration of complex branched shells of revolution: Analysis and user's Manual for BOSOR4, NASA CR-2116 (October 1972).

Абстракт — в первый раз дается краткое изложение схематических труд ностей и парадоксов вокруг анализа бифуркаций для пластического выпучивания. Кратко обсуждаются неконсервативность, скорость нагружения во время выпучивания и расхождения предсказаний выпучивания на основе теории пластического течения по сравнении с теорией пластической деформации. Дается резюме осесимметрического анализа до время потери устойчивости, при учете больших деформаций, упруго — пластического поведения материала и ползучести.

Приводятся подробности анализа несимметрической бифуркации из деформированного, осе-симметрического состояния. Описываются как теория пластического течения, так и теория деформации.

Применяется обсуждение, основанное на методе энергии в конечных разностях, к слоистым, сегментным и разветленным оболочкам, произвольной меридиональной Форме, составленных из числа разных упругопластических материалов.

Даются численные результаты, получены из программы вычислительной машины, для цилиндра с конической головкой под влиянием внешнего давления.